Heliyon 7 (2021) e08692

Contents lists available at ScienceDirect

Heliyon

journal homepage: www.cell.com/heliyon

Research article

Carbon-mixed dental cement for fixing fiber optic ferrules prevents visually triggered locomotive enhancement in mice upon optogenetic stimulation

Naozumi Araragi [a,b,*,1], Natalia Alenina [a,c], Michael Bader [a,b,d,e]

[a] Max Delbrück Center for Molecular Medicine in the Helmholtz Association, Robert-Rössle-Straße 10, 13125 Berlin, Germany
[b] Charité – Berlin University of Medicine, Charitéplatz 1, 10117 Berlin, Germany
[c] Institute of Translational Biomedicine, St. Petersburg State University, University Embankment 7-9, 199034 St. Petersburg, Russia
[d] German Center for Cardiovascular Research (DZHK), Partner Site Berlin, Germany
[e] Institute for Biology, University of Lübeck, Germany

HIGHLIGHTS

- Dental cement for fixating optic fiber ferrules was shown to permit light leakage.
- Such light leakage was quantified as photon counts.
- Leaked light induced locomotive enhancement through visual stimuli.
- By adding carbon to the dental cement mixture, such light leakage can be prevented.
- The method enables behavioral experiments without confounding visual factors.

ARTICLE INFO

Keywords:
Locomotion
Serotonin (5-HT)
Dental cement
Light leakage
Carbon

ABSTRACT

Optogenetics enables activation/silencing of specific neurons with unprecedented temporal and spatial resolution. The method, however, is prone to artefacts associated with biophysics of light used for illuminating opsin-expressing neurons. Here we employed Tph2-mhChR2-YFP transgenic mice, which express channelrhodopsin (ChR2) only in serotonergic neurons in the brain, to investigate behavioral effects of optogenetic stimulation of serotonergic neurons. Surprisingly, optogenetic stimulation enhanced locomotion even in ChR2-negative mice. Such unspecific effects are likely to be due to visual agitation caused by light leakage from the dental cement, which is commonly used to fixate optic fiber ferrules on the skull. When we employed black dental cement made by mixing carbons with dental cement powders, such unspecific effects were abolished in ChR2-negative mice, but not in ChR2-positive mice, confirming that enhanced locomotion resulted from serotonergic activation. The method allows extracting genuine behavioral effects of optogenetic stimulation without contamination from visual stimuli caused by light leakage.

1. Introduction

Behavior is an outcome of complex neural computation played by various cell types in the brain. For understanding neural mechanisms of behavior, it is thus important to be able to activate (or silence) specific neuronal subtypes. Optogenetics, in this sense, has been making great contributions since it enables activation (or silencing) of specific neurons by placing opsin genes under specific promoters. Excellent temporal and spatial resolution of optogenetics has made this method even more attractive for many behavioral neuroscientists. Using light to control neuronal activities, however, is not a natural phenomenon and may contaminate behavioral results through visual stimuli originating in the pathway from the light source till the implanted optic fiber in the brain. In our current study, we used Tph2-mhChR2-YFP transgenic mice, which express channel-rhodopsin (ChR2) exclusively in serotonin (5-HT) positive neurons (Zhao et al., 2011) as a model to investigate effects of optogenetic activation of serotonergic neurons on locomotion. Unexpectedly, we observed behavioral changes not only in ChR2-positive (ChR2+), but also

* Corresponding author.
E-mail address: naozumi.araragi@mdc-berlin.de (N. Araragi).
[1] Lead contact.

https://doi.org/10.1016/j.heliyon.2021.e08692
Received 6 October 2021; Received in revised form 29 November 2021; Accepted 27 December 2021

in wild type mice which do not express ChR2 (ChR2-). Such behavioral changes were manifested as locomotive enhancement in several parameters we measured. In particular, we measured how fast (velocity), how much (track length), and how often (activity) mice moved, as well as the geometric extent of mouse movement by counting zone crossing (ZC) and rated zone crossing (RZC), the latter of which focuses more on linear movement. We assumed that mice were visually agitated by light emanating through the dental cement used to fixate fiber optic ferrules on the skull. Indeed, rodents are quite sensitive to changes in brightness in the environment (Godsil and Fanselow, 2004). Sensitiveness to illumination may have developed as a defensive mechanism to detect potential predators approaching from above (Wei et al., 2015). Moreover, mice were shown to possess photoreceptors sensitive to blue light (Horibe et al., 2017; Peirson et al., 2018; Vicente-Tejedor et al., 2018). Several authors called attention in the design and interpretation of optogenetic behavioral experiments, taking into account possible artefacts caused by light leakage in the light delivery pathway (Ung and Arenkiel, 2012; Allen et al., 2015). There have been, however, only a few studies which addressed this issue in their behavioral experiments. Studies using rats showed that rats can acquire conditional fear by pairing footshock with faint light leakage from the dental cement, termed "caplight" (Eckmier et al., 2016), although locomotion was not or only marginally influenced by light leakage (Guo et al., 2014; Eckmier et al., 2016). In another study, Horibe and colleagues directly exposed mother mice and pups to blue LED without implementing optogenetics and saw no influence on maternal care or pups' brain function development, except that retinas of mother mice were damaged (Horibe et al., 2017). Importantly, those studies conducted in the darkness, which corresponds to the active phase of nocturnal animals such as mice, also reported no apparent influences on mice locomotive behaviors (Eckmier et al., 2016). In contrast to these previous reports, we observed that caplight did influence mouse locomotive behaviors, and replacing conventional dental cement with the one mixed with carbon abolishes such confounding influences from the caplight. Since we still saw enhanced locomotion with this method in ChR2+ mice, but not in ChR2-mice, we were able to conclude that enhanced locomotion was a genuine serotonergic effect. We therefore propose carbon-mixed dental cement as an appropriate method to eliminate unspecific visual agitation associated with optogenetic illumination and to extract genuine behavioral effects of neuronal subtypes targeted by optogenetic manipulation.

2. Materials and methods

2.1. Resource availability

2.1.1. Lead contact

Further information and requests for resources and reagents should be directed to and will be fulfilled by the lead contact, Naozumi Araragi (naozumi.araragi@mdc-berlin.de).

2.1.2. Materials availability

This study did not generate new unique reagents.

2.1.3. Data and code availability

Raw data from Figures 1 and 3 were deposited on Mendeley at https://doi.org/10.17632/fcngrmf29h.1. This paper does not report original code. Any additional information required to reanalyze the data reported in this paper is available from the lead contact upon request.

2.2. Experimental model and subject details

2.2.1. Animals

Animal handling and experiments followed national and institutional guidelines (Landesamt für Gesundheit und Soziales; LaGeSo) and were approved by the appropriate authorities. Animals were housed under a 12 h-light/dark cycle (lights on: 06:30–18:30) at ambient temperature of 22 ± 1 °C and a relative humidity of 40–50% with ad libitum access to food and water. Tph2-mhChR2-YFP transgenic mice were obtained from Jackson Laboratory (https://www.jax.org/strain/014555). This BAC transgenic mouse line expresses channelrhodopsin-2/enhanced yellow fluorescent protein – fusion protein (mhChR2:YFP) under the control of the tryptophan hydroxylase 2 (Tph2)-promotor, which is specific for serotonergic neurons (Zhao et al., 2011). Young adult female mice at the age of 6–8 weeks were used for experiments. ChR2-positive (ChR2+) and their wildtype (ChR2-) littermates were operated either with normal dental cement (see the next section) or with dental cement mixed with carbon (= black cement; BC) and further subjected to optogenetic stimulation (Stim+). ChR2+ mice, which were operated with normal dental cement and connected to optical patch cables but did not receive any light stimulation (Stim-), were used as a control group.

2.3. Method details

2.3.1. Optic fiber implantation

Mice were anesthetized with an intraperitoneal (i.p.) injection of ketamine and xylazine (100/10 mg/kg body weight). The deepness of anesthesia was controlled by tail-pinch. The scalp was shaved and disinfected with 70% isopropyl alcohol and 4% chlorhexidine digluconate (diluted from 20% solution; Caesar & Loretz GmbH, Hilden, Germany). The mouse was placed on an electric or warm water heating plate (37 °C) in a stereotaxic frame and its head was fixed. Eyes were covered with Bepanthen (Bayer, Leverkusen, Germany) or Visc-Ophtal (Dr. Robert Winzer Pharma GmbH, Berlin, Germany) to protect them from dryness. The scalp was incised along the midline and kept open with a retractor. The skull was then wiped with 3–6% H_2O_2 to form micropores (Ung and Arenkiel, 2012). The skull was drilled at three positions and small screws (Self-Tapping Bone Screws, 19010-10, Fine Science Tools GmbH, Heidelberg, Germany), which serve as anchors for dental cement, were screwed in. Then craniotomy was conducted above the median raphe nucleus (MRN). A stainless steel optic fiber ferrule (SFLC230-10, Thorlabs GmbH, Bergkirchen, Germany) with a 200 μm core, 0.66 NA fiber (Prizmatix, Holon, Israel) was inserted into the MRN (AP: -4.60 mm from the bregma, ML: +2.0 mm with an angle of 25°, DV: -4.45 mm). All the stereotaxic coordinates are based on Paxinos and Franklin (2004). The optic fiber ferrule was then fixed either with normal dental cement (Vertex Self-Curing Acrylic Powder, Shade: 8 (blue-pink) and Vertex Self-Curing Acrylic Liquid; Vertex Dental, Soesterberg, the Netherlands) or with BC (carbon 20 % w/w in powder mix: Sigma-Aldrich, Munich, Germany) on the skull (end weight after hardening ca. 0.5 g). Intraoperative and on the first postoperative day, mice were subcutaneously injected with carprofen (5 mg/kg body weight; Rimadyl, Pfizer Deutschland GmbH, Berlin, Germany) to minimize pain. In addition, bupivacain 0.25% (diluted from 0.5% solution; Jenapharm, Jena, Germany) was applied on the wound as a local analgesic. The animals recovered from an operation on a warmed plate until the effect of anesthesia disappeared. All the animals were single caged after the operation to prevent manipulation and damage to the implanted optic fiber ferrules from inmates. Control animals without light stimulation also underwent exactly the same operation as the stimulated animals.

2.3.2. Optogenetic light stimulation

One week after the surgery, mice were placed separately in Plexiglas cages (37.5 × 21.5 cm). Implanted optical fiber ferrules were connected with optical patch cables (200 μm core, 0.66 NA, stainless steel mono-coil wrap reinforcement; Plexon, Dallas, TX, USA), which were in turn connected with PlexBright Compact LED Modules attached to PlexBright Motorized Carousels (Plexon, Dallas, TX, USA). In order to minimize light emission in the free space, connection between ferrules and patch cables were achieved using metal sleeves (Prizmatix, Holon, Israel; see Figure 2C). Light stimulation (465 nm; blue) was driven by a PlexBright 4 Channel Optogenetic Controller (Plexon, Dallas, TX, USA). 10 mW (318 mW/mm^2) pulsed light stimulations (20 Hz, 15 ms pulse width) were given every 5 min for the duration of 30 s starting at 0:00 for 6.5 h.

2.3.3. Behavioral analysis

Animal behaviors were recorded from the midnight until the room light turned on (0:00–6:30) using CinePlex Behavioral Research System (Plexon, Dallas, TX, USA) under IR light (Model: MIRA II, Franz Video-Equipment, Winterhausen, Germany). Images were captured in 640 × 480 formats in 30 fps. Mouse movements in pre-recorded videos were tracked and analyzed with ViewerII software (Biobserve GmbH, Bonn, Germany) at every third frame. Peri-stimulus changes in velocity, track length, activity, zone crossing (ZC), and rated zone crossing (RZC) were calculated during 30 s blocks of pre-stimulation, stimulation, and post-stimulation at every 5-minute interval. The values were normalized by subtracting pre-stimulation values at each stimulation within the same animal. Data from complete inactivity, i.e. value = 0 at pre-stimulation, stimulation, and post-stimulation, were omitted from further analysis. Data from the control unstimulated group (ChR2+ Stim-) were analyzed in the same way.

Activity was scored when the animal moved at least 1.00 cm per second. ZC was calculated by dividing an animal cage into virtual 3 × 3 cm grids and the number of line crossing events was scored. In contrast to ZC, RZC implements a rating that emphasizes linear movement and dismisses small-scale locomotion. To calculate RZC, each line crossing was weighted by a discrete factor between zero and four. The factor was calculated by looking at the last three line-crossings, by which the distances from the first two to the last were summed up. The distances were expressed as the number of necessary line crossings to get from the starting zone to the final zone. Finally, one count was subtracted. Thereby track oscillations at only one zone's margin were leveled to zero (for all the details of behavioral parameters, see the Viewer manual).

2.4. Quantification and statistical analysis

2.4.1. Behavioral data

Data are expressed as the mean ± SEM unless otherwise stated. Five experimental groups were used in this study: ChR2+ Stim- (control group), ChR2+ Stim+, ChR2+ Stim+ BC, ChR2- Stim+, ChR2- Stim+ BC. Peri-stimulation behavioral changes were analyzed with repeated-measures two-way ANOVA by pairing „during" and "post-stimulation" values from the same animal. Data from the whole 30-second epoch were averaged. Fisher's LSD was applied to post-hoc multiple comparisons. Multiple comparisons were conducted only in comparison to the non-stimulated control group (ChR2+ Stim-). Moreover, changes in behavioral parameters in comparison to the pre-stimulation state were assessed using a one-sample *t*-test by setting the theoretical mean value at 0. Further, effectiveness of BC on suppressing unspecific behavioral changes was assessed using a one-way Student's *t*-test between normal pink dental cement and BC in the same genotype/experimental group, i.e. ChR2+ Stim+ vs. ChR2+ Stim+ BC and ChR2- Stim+ vs. ChR2- Stim+ BC. All the statistical tests were performed by GraphPad Prism (GraphPad Software, San Diego, CA, USA). Significance levels were set to $p = 0.05$.

2.4.2. Measurement of photon counts

Operated mice with a fiber optic ferrule and dental cement were anesthetized with an i.p. injection of ketamine and xylazine (100/10 mg/kg body weight). The deepness of anesthesia was controlled by tail-pinch. The mouse was placed on an electric or warm water heating plate (37 °C) in a stereotaxic frame and its head was fixed. Eyes were covered with Bepanthen (Bayer, Leverkusen, Germany) or Visc-Ophtal (Dr. Robert Winzer Pharma GmbH, Berlin, Germany) to protect them from dryness. The stereotaxic frame was then placed under a SliceScope Pro 6000 upright fixed microscope (Scientifica, Uckfield, UK) with a PLN4x/0.1 objective lens (Olympus, Tokyo, Japan). Implanted optical fiber ferrules were connected with optical patch cables (200 μm core, 0.66 NA), which were in turn connected with PlexBright Table-Top LED Modules (Plexon, Dallas, TX, USA). In order to minimize light emission in the free space, connection between ferrules and patch cables were achieved using metal sleeves (Prizmatix, Holon, Israel; Figure 2C). Continuous light stimulation (465 nm; blue) was given by a PlexBright LD-1 Single Channel LED Driver (Plexon, Dallas, TX, USA). Images from the dental cement on the skull were obtained using a SciCam Pro camera (Scientifica, Uckfield, UK) controlled by Ocular software version 2.0 (Teledyne Photometrics, Birmingham, UK). First, the light intensity was quantified in grey levels (ADU: analog to digital units). Then the grey levels were converted to electrons with the following formula:

$$\text{Electrons} = (\text{ADU} - \text{bias value}) * \text{gain}$$

The bias value and gain were obtained from the certificate of performance of the camera (bias = 100, gain = 0.77). Next, the photon counts were calculated based on the quantum efficiency (QE) of the camera, that is

$$\text{Photons} = 100/\text{QE} * \text{Electrons}$$

According to the spectral curve of the camera, QE at 465 nm (= wavelength of our optogenetic light) was 60.00 %. Electron counts were therefore multiplied by 1.67 (= 100/60.00 %) to produce photon counts.

2.4.3. Light intensity heat map

Images were obtained by a SciCam Pro camera (Scientifica, Uckfield, UK) mounted on a stereo microscope (Model Z850, Warner instruments, MA, USA) using a 0.5x C-mount adapter (Warner instruments, MA, USA). Image acquisition was controlled by Ocular software version 2.0 (Teledyne Photometrics, Birmingham, UK). Obtained images were loaded in ImageJ version 1.53e (Schneider et al., 2012) and converted to 8-bit images using the built-in function. Using HeatMap-Histogram plug-in (downloadable at http://www.samuelpean.com/heatmap-histogram), brightness values of the image were binned into 256 levels between minimum and maximum. A thermal LUT (Look-Up Table) was applied to visualize brightness in a thermal color scale.

3. Results

3.1. Light leakage from the dental cement during and post optogenetic stimulation facilitates locomotion

Behavioral changes during and post optogenetic stimulation in comparison to the pre-stimulation status are summarized in Figure 1 and Table 1. As evident here, all the parameters measured increased during and post the stimulation with respect to the pre-stimulation status in optogenetically stimulated (= Stim+) ChR2+ and ChR2- mice operated with normal dental cement. Behavioral facilitation was present in comparison to both the control group without optogenetic stimulation (ChR2+ Stim-) and their own pre-stimulation values (normalized to 0). Notably, black cement (BC) prevented enhanced locomotion in the ChR2- Stim+ group but not in the ChR2+ Stim+ group. Given that ChR2- mice do not express any opsins, our results suggest that enhanced locomotion observed in the ChR2- Stim+ group was caused by light leakage from the normal dental cement. It is presumable that this light leakage visually agitated mice and led to enhanced locomotion. BC effectively prevented this visually evoked locomotive enhancement. Indeed, behavioral patterns of ChR2- Stim+ BC mice were almost identical to those of non-stimulated mice (ChR2+ Stim-). Enhanced locomotion observed in the ChR2+ Stim+ BC, on the other hand, is likely to be due to genuine effects of optogenetic stimulation of serotonergic neurons since there was practically no light leakage from the dental cement (see the next section) in this group. In line with this, behavioral facilitation was evident not only during stimulation but also lasted or further increased in the post-stimulation period in ChR2-positive stimulated groups (i.e., ChR2+ Stim+ and ChR2+ Stim+ BC). In ChR2- Stim+ group, on the other hand, behavioral facilitation was more pronounced during the light stimulation

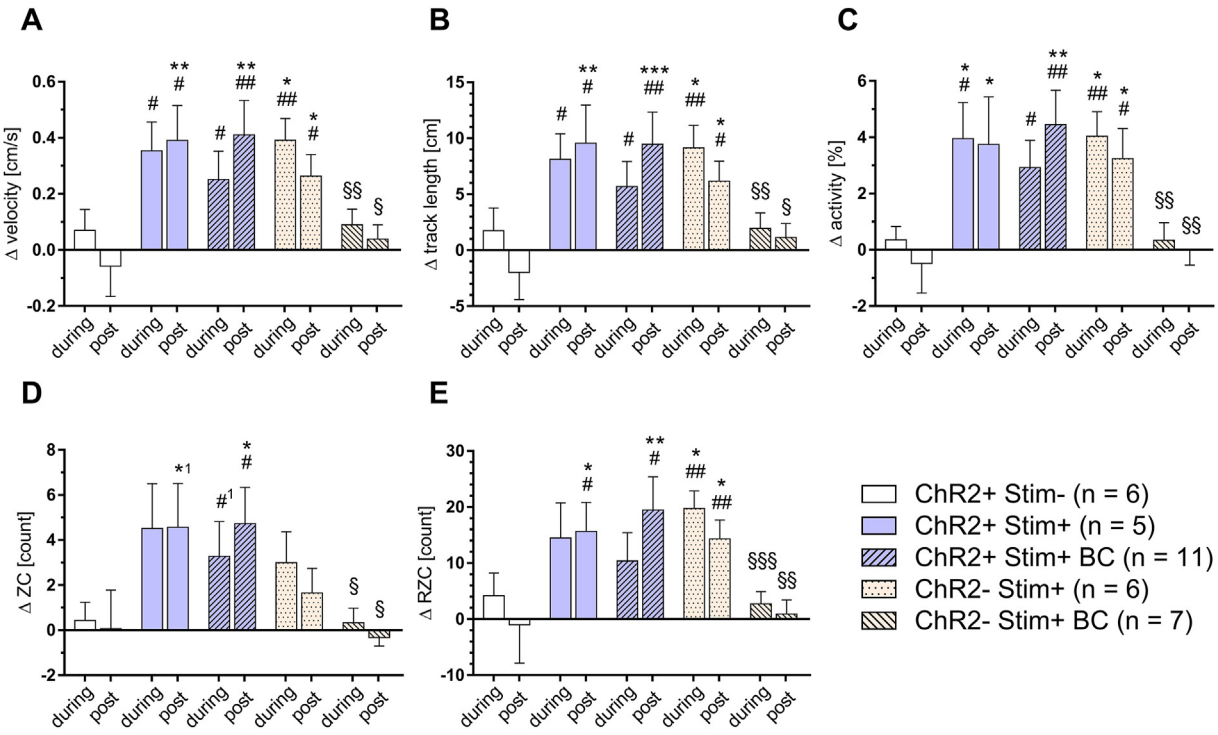

Figure 1. Light leakage from the dental cement during and post optogenetic stimulation facilitates locomotion. Behavioral data from median raphe nucleus (MRN) overnight stimulation with normal dental cement and carbon-mixed black cement (BC) are summarized here. Averaged changes of velocity (A), track length (B), activity (C), zone crossing (ZC; D), and rated zone crossing (RZC; E) at night (0:00–6:30 h). Data were collected during the 30-second stimulation period (during) and preceding (pre) and succeeding (post) 30-second periods. Data were normalized by subtracting pre values of each animal, at each light stimulation. Data are presented as mean + SEM. n = number of animals. $^{*}p \leq 0.05$, $^{**}p \leq 0.01$, $^{***}p \leq 0.001$, $^{*1}p = 0.06$; two-way repeated measures ANOVA and the Fisher's LSD multiple comparison test, compared to the control group (i.e. ChR2+ Stim-) within the same experimental period, i.e. (during/post-)stimulation. $^{\#}p \leq 0.05$, $^{\#\#}p \leq 0.01$, $^{\#1}p = 0.06$; one-sample *t*-test, compared to the pre-stimulation value (= 0) in the same group. $^{\S}p \leq 0.05$, $^{\S\S}p \leq 0.01$, $^{\S\S\S}p \leq 0.001$; one-way Student's *t*-test, comparison between the normal cement and the corresponding BC group, i.e. ChR2+ Stim+ vs. ChR2+ Stim+ BC or ChR2- Stim+ vs. ChR2- Stim+ BC. Abbreviations; ChR2+: mice with channelrhodopsin (ChR2) expression, ChR2-: mice without ChR2 expression, Stim+: mice with optogenetic stimulation, Stim-: mice without optogenetic stimulation. Numerical results are presented in Table 1.

than post-stimulation, indicating direct influence of visual stimulation. Prolonged or even accentuated behavioral facilitation observed in the post-stimulation period of ChR2+ mice may reflect delayed effects of released and accumulated neurotransmitter 5-HT.

Behavioral facilitation measured as ZC in light stimulated groups was less pronounced compared to RZC. Since high ZC values could have resulted simply because of minimal but frequent positional changes in the close vicinity of a zone grid line, more pronounced increase in RZC

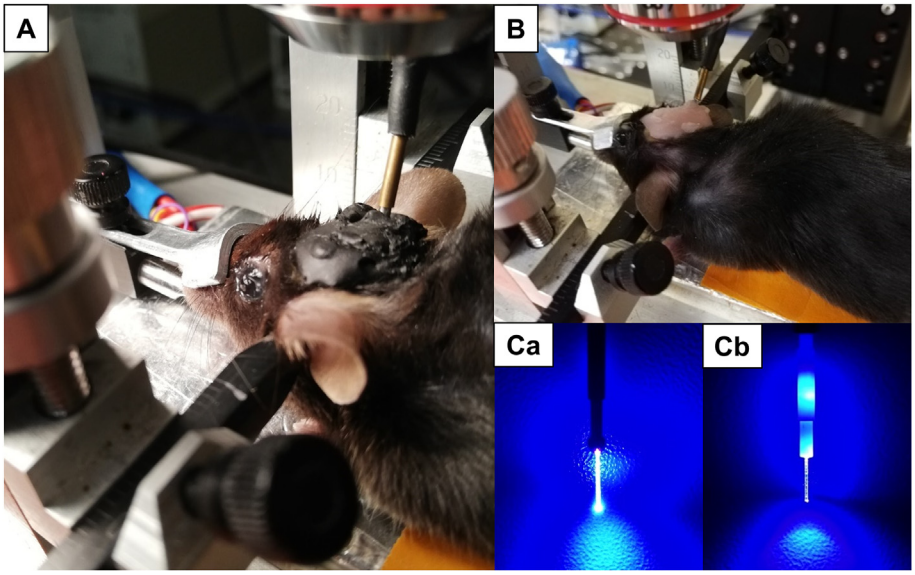

Figure 2. Experimental setup for photon counts measurement. (A, B) Operated mice with black or normal (pink) cement. Mouse with black cement (A) or pink cement (B) was anesthetized with ketamine/xylazine, fixed in a stereotaxic apparatus, and placed under a microscope to measure light leakage. Eyes were protected by ointment and the body temperature was maintained by a warming plate. (C) Use of metal ferrules and sleeves (Ca) further prevents light leakage compared with ceramic ferrules and sleeves (Cb). Light output power from the patch cable was ca. 20 mW.

indicates that behavioral facilitation by light stimulation was more reflected as an increase in linear movement, not in small-scale locomotion.

In sum, our results show that mice are visually sensitive to blue light and using BC as a fixation method for fiber optic ferrules allows us to eliminate stray blue light leakage from the dental cement. This in turn prevents unspecific behavioral effects caused by visual agitation and allows for extracting only biological responses resulting from opsin activation.

3.2. Carbon-mixed black dental cement prevents light leakage

We then quantified light leakage from dental cement by placing mice under a microscope and giving optogenetic stimuli (Figure 2). In our experiments, we used metal ferrules and sleeves, which further prevented light leakage in comparison to those made of ceramics (Figure 2C; see Discussion). Figure 3A, B show image histograms obtained from an area (ca. 8.9 mm × 6.6 mm size) next to the optic fiber ferrule implantation when maximum intensity of optogenetic light stimulation (ca. 15 mW) was applied. As shown here, the image obtained from black cement contained almost no photons (mean photon count = 154.91, pixel peak at photon count = 0), whereas the image from pink cement showed a wide photon distribution (mean photon count = 6345.57, pixel peak at photon count = 3843). Figure 3C shows mean photon counts measured in the same area as Figure 3A, B as a function of increasing optogenetic light intensity. As evident here, the light leakage from pink dental cement, presented as photon counts, linearly increased with increasing intensity of light stimulation (photon = 347.5 * light intensity + 943.3, R^2 = 0.996, $F(1,7) = 1745$, $^{***}p \leq 0.001$, slope significantly different from zero). On the contrary, photon counts remained nearly zero regardless of light intensity in the case of black cement (photon = 0.9004 * light intensity + 119.1, $R^2 = 0.183$, $F(1,7) = 1.57$, $p = 0.25$, slope not significantly different from zero). Slopes of two regression lines were significantly different ($F(1,14) = 1690$, $^{***}p \leq 0.001$).

Next, photon counts were measured as a factor of increasing distance from the midline on the skull (Figure 3D). In the case of pink cement, the photon counts non-linearly ($^{***}p \leq 0.001$, Runs test; significantly deviated from linearity) decreased and maintained relatively low level of photon counts away from the midline on the skull. Indeed, the decrease in photon counts were best fitted by non-linear regression: photon = 4288 + (18840 - 4288)*exp.$^{-0.00246*\text{distance}}$, one-phase decay, R^2 = 0.966. On the other hand, black cement did not allow any light leakage and there was no clear pattern of photon count transition as a factor of distance from the midline. As expected, the maximum photon counts reached (ca. 18,000 in pink cement, ca. 1,000 in black cement) correspond to the maximum photon counts observed in the photon distribution histograms as shown in Figure 3A, B.

Finally, extent of light emission in space was visualized as a heat map on the dental cement (Figure 3E, F). Here, light intensity was scaled into 256 levels and color-coded. When the pink dental cement was used (Figure 3Ea, Eb), light leakage was strongest near the midline next to the implanted optic fiber ferrule and gradually diminished sideways. This is probably due to the fact that we targeted the MRN, which is located in the median plane of the brain. On the contrary, there was practically no light leakage from the black cement regardless of the light intensities (Figure 3Fa, Fb).

In sum, black cement permitted almost no light leakage, independent of light stimulation intensity or location from the implanted fiber optic ferrule. Contrarily, pink cement permitted light leakage and its magnitude increased linearly to the stimulation intensity. Spatial dispersion of light leakage on the surface of pink dental cement can be modeled as an exponential decay from the targeted site of optogenetic stimulation.

4. Discussion

Unspecific behavioral effects, i.e. effects which can be observed even in the absence of opsins, induced by light leakage in optogenetic experimental setups have been often underestimated and there have been only a few studies which directly addressed this issue (Guo et al., 2014; Eckmier et al., 2016). Nonetheless, several authors suggested various methods to minimize light leakage in order to prevent unintended potential behavioral effects of light leakage. For example, Ung and Arenkiel proposed to cover ceramic ferrule sleeves with heat-shrink tubing (Ung and Arenkiel, 2012). The disadvantage of this method, however, is that it also covers the sleeve slit which provides visual feedback for checking tight contact between the tip of patch cables and ferrules. In such a case, tight contact can only be confirmed with tactile feedback. Moreover ceramic sleeves and ferrules are translucent and more prone to light leakage (Eckmier et al., 2016). As opposed to ceramics, metals are not

Table 1. Numerical results corresponding to Figure 1. Values are means ± SEM. n = number of animals. $^{*}p \leq 0.05$, $^{**}p \leq 0.01$, $^{***}p \leq 0.001$, $^{*1}p = 0.06$; two-way repeated measures ANOVA and the Fisher's LSD multiple comparison test, compared to the control group (i.e. ChR2+ Stim-) within the same experimental period, i.e. (during/post-)stimulation. F-values are shown at the right of the table. Group = five experimental groups defined by combination of genotype, with/without light stimulation, and the type of dental cement. Time = during or post-stimulation. $^{\$}p \leq 0.05$, $^{\$\$}p \leq 0.01$. G × T = Group × Time interaction effect. $\#p \leq 0.05$, $\#\#p \leq 0.01$, $^{\#1}p = 0.06$; one-sample *t*-test, compared to the pre-stimulation value (= 0) in the same group. $^{\S}p \leq 0.05$, $^{\S\S}p \leq 0.01$, $^{\S\S\S}p \leq 0.001$; one-way Student's *t*-test, comparison between the normal cement and the corresponding black cement (BC) group, i.e. ChR2+ Stim+ vs. ChR2+ Stim+ BC or ChR2- Stim+ vs. ChR2- Stim+ BC. See Figure 1 legend for abbreviations.

Variable	ChR2+ Stim- (n = 6)		ChR2+ Stim+ (n = 5)		ChR2+ Stim+ BC (n = 11)		ChR2- Stim+ (n = 6)		ChR2- Stim+ BC (n = 7)		*F*(DFn, DFd) and *p* value		
	during	post	during	post	during	post	during	post	during	post	Group *F*(4,30)	Time *F*(1,30)	G × T *F*(4,30)
Δvelocity	0.07 ± 0.07	-0.06 ± 0.11	0.35 ± 0.10 #	0.39 ± 0.12 **, #	0.25 ± 0.10 #	0.41 ± 0.12 **, ##	0.39 ± 0.08 *, ##	0.26 ± 0.08 *, #	0.09 ± 0.06 §§	0.04 ± 0.05 §	3.24 $^{\$}p = 0.03$	0.26 $p = 0.61$	2.11 $p = 0.10$
Δtrack length	1.75 ± 2.03	-1.97 ± 2.43	8.13 ± 2.28 #	9.56 ± 3.42 **, #	5.69 ± 2.24 #	9.46 ± 2.88 ***, ##	9.15 ± 2.01 *, ##	6.17 ± 1.78 *, #	1.97 ± 1.38 §§	1.15 ± 1.24 §	3.30 $^{\$}p = 0.02$	0.20 $p = 0.66$	2.22 $p = 0.09$
Δactivity	0.36 ± 0.47	-0.48 ± 1.06	3.95 ± 1.29 *, #	3.74 ± 1.70 *	2.93 ± 0.97 #	4.45 ± 1.22 **, ##	4.04 ± 0.88 *, ##	3.25 ± 1.06 *, #	0.33 ± 0.63 §§	-0.01 ± 0.53 §§	4.20 $^{\$\$}p = 0.008$	0.09 $p = 0.76$	1.39 $p = 0.26$
ΔZC	0.44 ± 0.79	0.06 ± 1.72	4.51 ± 1.99	4.57 ± 1.94 *1	3.28 ± 1.55 #1	4.73 ± 1.61 *, #	2.99 ± 1.38	1.66 ± 1.09	0.33 ± 0.65 §	-0.32 ± 0.39 §	2.37 $p = 0.08$	0.08 $p = 0.77$	0.82 $p = 0.52$
ΔRZC	4.19 ± 4.02	-1.01 ± 6.83	14.48 ± 6.28	15.65 ± 5.15 *, #	10.37 ± 5.04	19.47 ± 5.90 **, #	19.74 ± 3.15 *, ##	14.30 ± 3.39 *, ##	2.71 ± 2.19 §§§	0.93 ± 2.49 §§	2.67 $^{\$}p = 0.05$	0.04 $p = 0.84$	2.30 $p = 0.08$

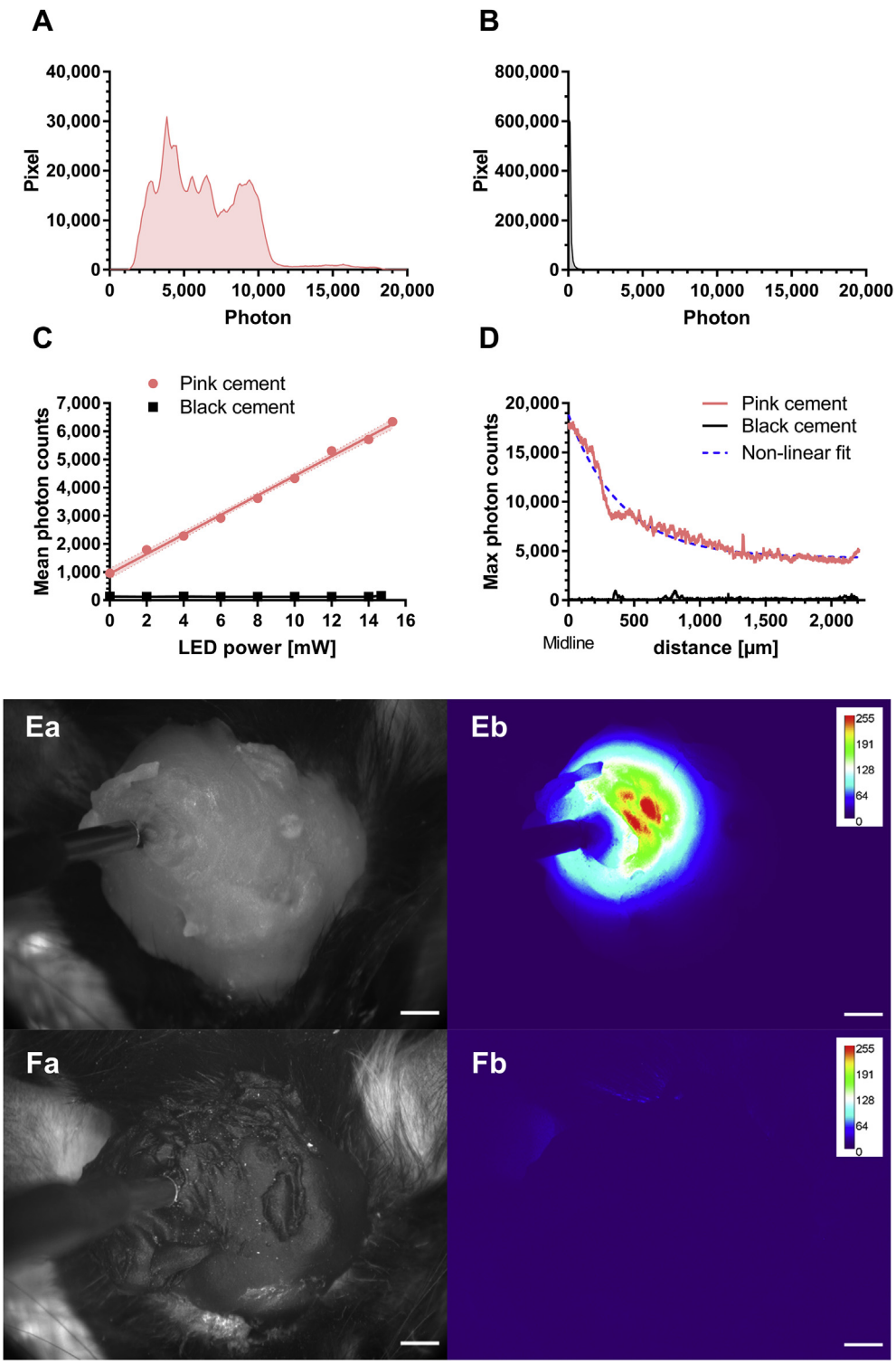

Figure 3. Carbon-mixed black dental cement prevents light leakage. Light leakage was quantified as photon counts. Image histograms from the pink cement (A) or black cement (B) when the maximum intensity of light stimulation (ca. 15 mW from the ferrule tip) was given. Pixel counts are presented as areas under the curve. (C) Relationship between light output intensity and the mean photon counts measured from the light leakage. LED power corresponds to the end light output intensity from the tip of implanted fiber optic ferrules based on the light transmission efficiency (ca. 75%) measured before implantation. A linear regression plot is shown for pink cement data with a 95% confidence band of the slope. (D) Maximum photon counts as a function of distance from the implanted fiber optic ferrule with the light intensity of 15 mW. 0 in the x-axis corresponds to the midline on the skull and the maximum photon counts are plotted toward the direction away from the implanted fiber optic ferrule. Blue dotted curve shows a best-fitted exponential decay curve obtained from non-linear regression analysis for pink cement data (see Results for the equation). (E, F) Heat map images showing extent of light leakage. Figures on the left were taken in the brightness without optogenetic stimulation to show images of the whole dental cement (pink: Ea, black: Fa) on the skull. Heat maps (pink: Eb, black: Fb) are scaled in relative intensity by taking the complete darkness outside of the cement as 0 and the maximum brightness as 255 when 15 mW optogenetic stimulation was given. Scale bar (bottom right) = 2 mm.

translucent and do not permit light leakage. In our study, we used both metal sleeves and ferrules to suppress light leakage. The advantage of metal sleeves is that they maintain slits for visual inspection of tight coupling between patch cables and ferrules, while light leakage from such slits is negligible. Another author delivered a series of bright blue light flashes as a visual distractor to the behavioral arena to mask possible scattered light from the optogenetic stimulation (Huber et al., 2008). In addition, it was suggested that experimenters choose wavelengths of light that the animals cannot see or are less responsive to, as well as use animals that are engineered to be insensitive to light (Allen et al., 2015). Using a commercially available dark-colored acrylic resin could also be an option to reduce light leakage (Correia et al., 2017). All these methods, however, depend on the availability of products, devices or animals and are not necessarily easily implementable. The method we presented with black dental cement is easily implementable and yet can effectively prevent light leakage and its associated unspecific behavioral effects. Mixing carbon with dental cement was successfully applied in imaging studies to prevent light scatter which may disturb acquisition of

images (Zhang et al., 2019). Our study is unique in that it applied black cement in behavioral studies and directly compared behavioral influences from light leakage between normal dental cement (usually pink) and black cement. Furthermore, we quantified light leakage in photon counts and objectively demonstrated that black dental cement can almost completely prevent light leakage.

The light intensity and irradiance we used for our behavioral experiments, i.e. 10 mW (318 mW/mm^2) is common in behavioral experiments utilizing optogenetic stimulation and was used in other studies stimulating serotonergic neurons in raphe nuclei (Dugué et al., 2014; Teixeira et al., 2018). It should be noted that, although the minimal light intensity required for activating ChR2-expressing neurons is in the order of 1 mW/mm^2 (Wang et al., 2012), *in vivo* optogenetic light is typically delivered to the tissue at 100-fold or more higher intensity than required at the target cell in order to compensate for scattering losses inside the tissue (Yizhar et al., 2011). Results from photon count measurements confirmed that our carbon-mixed dental cement method effectively prevents light leakage up to the maximum light intensity we tested (15 mW; 477 mW/mm^2). Although not directly tested in our study, our method to prevent light leakage could be also useful for transcranial optogenetic light illumination, where high intensity of light (typically >200 mW/mm^2) is required (Chen et al., 2021).

There is a possibility that optogenetic light propagates inside the brain and reaches the back of the retina, causing visually triggered behavioral artefacts. This was shown to be more often the case when the optogenetic stimulation was conducted by red light, compared to blue light (Danskin et al., 2015). This is because long wavelength light penetrates better in the tissue than short wavelength light. Indeed, it was shown that blue light is particularly prone to intensity attenuation in the brain tissue (Aravanis et al., 2007; Yizhar et al., 2011; Stark et al., 2012). In our study, we implanted an optic fiber in the MRN (AP: -4.60 mm from the bregma, ML: +2.0 mm with an angle of 25°, DV: -4.45 mm). The distance between the optic fiber insertion site and the retina is about 7.9 mm on the ipsilateral side and 9.2 mm on the contralateral side (measurement based on Danskin et al., 2015). The light intensity we used (10 mW; 318 mW/mm^2) attenuates already to 0.01 mW/mm^2 after propagating for 2.45 mm inside the brain (source: http://web.stanford.edu/group/dlab/cgi-bin/graph/chart.php; with a 200 μm core, 0.66 NA fiber). Therefore, it can be reasonably assumed that the light intensity becomes practically 0 before it reaches the retina. This supports the assumption that the enhanced locomotion was due to visual agitation caused by light leakage from the dental cement, not by the light propagation inside the brain and the resultant direct activation of the retina from the back of the eye.

In the current study, we used Tph2-mhChR2-YFP transgenic mice to investigate how optogenetic stimulation of serotonergic neurons influences locomotion. Our results showed that stimulating serotonergic neurons in the MRN facilitates locomotion, which corresponds with previous reports from others (Balázsfi et al., 2017; Gölöncsér et al., 2017; Teixeira et al., 2018). Importantly, enhanced locomotion was observed in the ChR2+ Stim+ BC group, too, confirming that this behavioral enhancement was not caused by visual agitation. Indeed, previous studies demonstrated that ascending serotonergic projections play an important role in such motor activities as walking, changing posture, or moving the head about, resulting in enhanced locomotion in general (Gölöncsér et al., 2017). Alternative hypothesis is that MRN stimulation is perceived as unpleasant aversive stimuli like electric shocks. This may have resulted in shock-induced runs, i.e. sudden increase in locomotive activities (Balázsfi et al., 2017). In line with this, it was shown that MRN stimulation resulted in activation of neural regions involved in the processing of stress and aversive stimuli (Balázsfi et al., 2017). Given this, it is important to eliminate experimental artefacts which may cause behavioral agitation, such as light leakage from the dental cement and its associated visual agitation. It is often the case, however, that normal dental cement was used for fixing fiber optic ferrules or the method section of publication does not clearly mention what kind of dental cement was used in the experiments. Thus, caution should be taken in interpretation and implementation of optogenetic behavioral experiments, especially when they were conducted in the darkness. Of course, light leakage from the dental cement is less interfering when experiments are conducted in brightness. This, however, may negatively influence behaviors of nocturnal animals such as rodents since they are more active in the darkness. For such animals, it is necessary to measure locomotive activities in the darkness and at the same time minimize light leakage when optogenetic methods are employed. The black cement method we presented here is easy to implement and yet highly effective in preventing light leakage, allowing behavioral experiments with minimum confounding factors.

5. Limitations of the study

The present study focused on methodological aspects of optogenetic experiments in order to eliminate visually triggered unspecific locomotive enhancement. We, therefore, did not directly investigate the underlying neuronal circuit which led to visually induced enhanced locomotion through light leakage. Similarly, we did not address the question, how optogenetic activation of serotonergic neurons led to enhanced locomotion. Further studies are therefore needed to reveal neuronal mechanisms of visually triggered and serotonin-induced locomotive enhancement. Another limitation of the study is that we did not test the effectiveness of our method for light at different wavelengths, for example, yellow and red light. Nonetheless, with these colors, influence of leaked light on behavior is expected to be smaller than that of blue light, since the visual sensitivity of mice steeply declines with increasing wavelengths across the visible spectrum. For light at longer wavelengths, propagation of light through the brain tissue and resultant direct activation of the retina from the back of the eye is more problematic (Danskin et al., 2015). Our method does not provide a direct solution to prevent this problem.

Declarations

Author contribution statement

Naozumi Araragi: Conceived and designed the experiments; Performed the experiments; Analyzed and interpreted the data; Contributed reagents, materials, analysis tools or data; Wrote the paper.

Natalia Alenina, Michael Bader: Conceived and designed the experiments; Contributed reagents, materials, analysis tools or data.

Funding statement

This work was supported by a fellowship from the European Molecular Biology Organization (EMBO, Grant ASTF 72-2014) to Natalia Alenina, by the project 73022475 of the St. Petersburg State University to Natalia Alenina, and by the EU H2020 MSCA ITN project “Serotonin and Beyond” (N 953327) to Natalia Alenina and Michael Bader.

Data availability statement

Data associated with this study has been deposited on Mendeley under the url: https://data.mendeley.com/datasets/fcngrmf29h/draft?a=7d462759-1642-4797-9590-56b1c409d371 or https://doi.org/10.17632/fcngrmf29h.1.

Declaration of interests statement

The authors declare no conflict of interest.

Additional information

No additional information is available for this paper.

Acknowledgements

We are grateful to Teledyne Photometrics (Birmingham, UK) for their technical support in measuring photon counts.

References

Allen, B.D., Singer, A.C., Boyden, E.S., 2015. Principles of designing interpretable optogenetic behavior experiments. Learn. Mem. 22, 232–238.

Aravanis, A.M., Wang, L.-P., Zhang, F., Meltzer, L.A., Mogri, M.Z., Schneider, M.B., Deisseroth, K., 2007. An optical neural interface: in vivo control of rodent motor cortex with integrated fiberoptic and optogenetic technology. J. Neural. Eng. 4, S143–S156.

Balázsfi, D.G., Zelena, D., Farkas, L., Demeter, K., Barna, I., Cserép, C., Takács, V.T., Nyíri, G., Gölöncsér, F., Sperlágh, B., Freund, T.F., Haller, J., 2017. Median raphe region stimulation alone generates remote, but not recent fear memory traces. PLoS One 12, e0181264.

Chen, R., Gore, F., Nguyen, Q.-A., Ramakrishnan, C., Patel, S., Kim, S.H., Raffiee, M., Kim, Y.S., Hsueh, B., Krook-Magnusson, E., Soltesz, I., Deisseroth, K., 2021. Deep brain optogenetics without intracranial surgery. Nat. Biotechnol. 39, 161–164.

Correia, P.A., Matias, S., Mainen, Z.F., 2017. Stereotaxic adeno-associated virus injection and cannula implantation in the dorsal raphe nucleus of mice. Bio-protocol 7 e2549-e2549.

Danskin, B., Denman, D., Valley, M., Ollerenshaw, D., Williams, D., Groblewski, P., Reid, C., Olsen, S., Blanche, T., Waters, J., 2015. Optogenetics in mice performing a visual discrimination task: measurement and suppression of retinal activation and the resulting behavioral artifact. PLoS One 10, e0144760.

Dugué, G.P., Lörincz, M.L., Lottem, E., Audero, E., Matias, S., Correia, P.A., Léna, C., Mainen, Z.F., 2014. Optogenetic recruitment of dorsal raphe serotonergic neurons acutely decreases mechanosensory responsivity in behaving mice. PLoS One 9, e105941.

Eckmier, A., Daney de Marcillac, W., Maître, A., Jay, T.M., Sanders, M.J., Godsil, B.P., 2016. Rats can acquire conditional fear of faint light leaking through the acrylic resin used to mount fiber optic cannulas. Learn. Mem. 23, 684–688.

Godsil, B.P., Fanselow, M.S., 2004. Light stimulus change evokes an activity response in the rat. Anim. Learn. Behav. 32, 299–310.

Gölöncsér, F., Baranyi, M., Balázsfi, D., Demeter, K., Haller, J., Freund, T.F.F., Zelena, D., Sperlágh, B., 2017. Regulation of hippocampal 5-HT release by P2X7 receptors in response to optogenetic stimulation of median raphe terminals of mice. Front. Mol. Neurosci. 10, 325.

Guo, S., Chen, S., Zhang, Q., Wang, Y., Xu, K., Zheng, X., 2014. Optogenetic activation of the excitatory neurons expressing CaMKIIα in the ventral tegmental area upregulates the locomotor activity of free behaving rats. BioMed Res. Int. 2014, 687469.

Horibe, M., Yoshino, Y., Domoto, S., Nakamura, M., Shimazawa, M., Hara, H., 2017. The effects of blue LED light on behavior and retinal function in maternal and offspring mice. JBBS 7, 348–359.

Huber, D., Petreanu, L., Ghitani, N., Ranade, S., Hromádka, T., Mainen, Z., Svoboda, K., 2008. Sparse optical microstimulation in barrel cortex drives learned behaviour in freely moving mice. Nature 451, 61–64.

Paxinos, G., Franklin, K.B.J., 2004. The Mouse Brain in Stereotaxic Coordinates, second ed. Acad. Press, San Diego, Calif.

Peirson, S.N., Brown, L.A., Pothecary, C.A., Benson, L.A., Fisk, A.S., 2018. Light and the laboratory mouse. J. Neurosci. Methods 300, 26–36.

Schneider, C.A., Rasband, W.S., Eliceiri, K.W., 2012. NIH Image to ImageJ: 25 years of image analysis. Nat. Methods 9, 671–675.

Stark, E., Koos, T., Buzsáki, G., 2012. Diode probes for spatiotemporal optical control of multiple neurons in freely moving animals. J. Neurophysiol. 108, 349–363.

Teixeira, C.M., Rosen, Z.B., Suri, D., Sun, Q., Hersh, M., Sargin, D., Dincheva, I., Morgan, A.A., Spivack, S., Krok, A.C., Hirschfeld-Stoler, T., Lambe, E.K., Siegelbaum, S.A., Ansorge, M.S., 2018. Hippocampal 5-HT input regulates memory formation and schaffer collateral excitation. Neuron 98, 992–1004 e4.

Ung, K., Arenkiel, B.R., 2012. Fiber-optic implantation for chronic optogenetic stimulation of brain tissue. J. Visual. Exp.: JoVE, e50004.

Vicente-Tejedor, J., Marchena, M., Ramírez, L., García-Ayuso, D., Gómez-Vicente, V., Sánchez-Ramos, C., de La Villa, P., Germain, F., 2018. Removal of the blue component of light significantly decreases retinal damage after high intensity exposure. PLoS One 13, e0194218.

Wang, J., Wagner, F., Borton, D.A., Zhang, J., Ozden, I., Burwell, R.D., Nurmikko, A.V., van Wagenen, R., Diester, I., Deisseroth, K., 2012. Integrated device for combined optical neuromodulation and electrical recording for chronic in vivo applications. J. Neural. Eng. 9, 16001.

Wei, P., Liu, N., Zhang, Z., Liu, X., Tang, Y., He, X., Wu, B., Zhou, Z., Liu, Y., Li, J., Zhang, Y., Zhou, X., Xu, L., Chen, L., Bi, G., Hu, X., Xu, F., Wang, L., 2015. Processing of visually evoked innate fear by a non-canonical thalamic pathway. Nat. Commun. 6, 6756.

Yizhar, O., Fenno, L.E., Davidson, T.J., Mogri, M., Deisseroth, K., 2011. Optogenetics in neural systems. Neuron 71, 9–34.

Zhang, L., Liang, B., Barbera, G., Hawes, S., Zhang, Y., Stump, K., Baum, I., Yang, Y., Li, Y., Lin, D.-T., 2019. Miniscope GRIN lens System for calcium imaging of neuronal activity from deep brain structures in behaving animals. Curr. Prot. Neurosci. 86, e56.

Zhao, S., Ting, J.T., Atallah, H.E., Qiu, Li, Tan, J., Gloss, B., Augustine, G.J., Deisseroth, K., Luo, M., Graybiel, A.M., Feng, G., 2011. Cell type–specific channelrhodopsin-2 transgenic mice for optogenetic dissection of neural circuitry function. Nat. Methods 8, 745–752.